International Journal of Power Electronics and Drive System (IJPEDS)
Vol. 7, No. 3, September 2016, pp. 665~676
ISSN: 2088-8694, DOI: 10.11591/ijpeds. v7.i3.pp665-676

Self-Tuning Fuzzy Based PI Controller for DFIM Powered by Two Matrix Converters

Abdelhakim Alalei[1], Abdeldjebar Hazzab[2], Ali Nesba[3]
[1,2] Laboratoire Commande, Analyse et Optimisation des Systèmes Electro-Energétiques, Université de Bechar, Algérie
[3] Laboratoire des Systèmes Intégrés à base de Capteurs, Ecole Normale Supérieure de Kouba, Alger, Algérie

Article Info

Article history:

Received Nov 12, 2015
Revised Mar 10, 2016
Accepted Apr 11, 2016

Keyword:

Adaptive PI controller
Doubly fed induction machine
Field oriented control
Fuzzy logic
Matrix converter

ABSTRACT

This paper presents a study of the Doubly Fed Induction Machine (DFIM) powered by two matrix converters; one connected to the stator windings and the other connected to the rotor windings. First, the mathematical model of DFIM and those of the matrix converters are developed. Then, the vector control technique is applied to the DFIM. Fuzzy logic is used in order to automatically adjust the parameters of the PI controller. The performance of this structure under different operating conditions is studied. Particular interest is given to the robustness of the fuzzy logic based control. The operation of the DFIM under overload conditions is also examined. Simulation results obtained in MATLAB/Simulink environment are presented and discussed.

Corresponding Author:

Abdeldjebar Hazzab,
Laboratoire Commande, Analyse et Optimisation des Systèmes Electro-Energétiques,
BP 417 route de Kenadsa,
Université de Bechar, Algérie.
Email: a_hazzab@yahoo.fr

1. INTRODUCTION

Recent years have seen a rapidly growing interest in the doubly fed induction machine (DFIM) due to the numerous advantages offered by this machine compared to other electrical machines. One of these advantages is the accessibility of its rotor, and thus the possibility to control this machine as well from the stator side than from the rotor side and the possibility of dispatching the active power between stator and rotor sides. Another benefit consists in the possibility of under sizing by one third the rotor side converter while taking advantage of the full power of the machine [1]. One can also quote that under certain conditions the active power of DFIM can be doubled. All these benefits and many others have led to wide use of this machine. For example, nearly 50% of the wind turbines installed today are equipped with doubly fed induction generators (DFIG) [2]-[4]. This is because the doubly fed induction generator can be operated over a wide range of wind speed leading to continuously extracting the maximum possible power [5], [6]. Besides, the DFIM is also used in a multitude of variable speed drive systems [7]. In this operating mode, the DFIM presents many advantages as well.

In the present paper, the DFIM powered by two matrix converters is studied (Figure 1). Matrix converters are chosen instead of the conventional VSI inverters because of their attractive benefits [8]-[11]. These benefits include: low harmonic distortion of the input currents (compared to conventional VSI), reduced size/weight, higher reliability and extended life span (due to DC bus elimination). In addition, the use of a matrix converter on the rotor side is more advantageous over a conventional voltage source inverter, in case of voltage sags. The speed and torque control is ensured by using the vector control technique along with an adaptive controller, namely, a fuzzy logic (FLC) based PI controller. The DFIM powered by two matrix converters is studied here because we found that this subject as defined in the present paper is sparsely documented in the scientific literature.

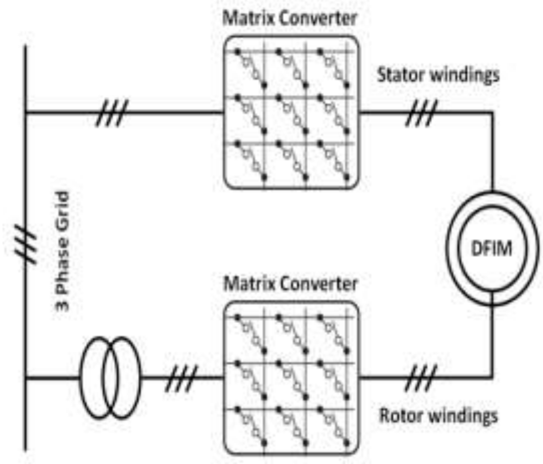

Figure 1. DFIM powered by two matrix converters

This paper is organized as follows. In the subsequent section the doubly fed induction machine model and the matrix converter model are set forth. The third section is devoted to the control of the DFIM, where the field oriented control technique, as well as the fuzzy logic based PI controller, are presented. The forth section presents and discusses the obtained results, with special focus on robustness test and on the operation of the DFIM beyond its nominal power.

List of symbols

V_{sd}, V_{sq}	Direct and quadrature stator voltages
V_{rd}, V_{rq}	Direct and quadrature rotor voltages
I_{sd}, I_{sq}	Direct and quadrature stator currents
I_{rd}, I_{rq}	Direct and quadrature rotor currents
Φ_{sq}, Φ_{sd}	Direct and quadrature stator fluxes
Φ_{rq}, Φ_{rd}	Direct and quadrature rotor fluxes
Φ_s	Stator fluxes
T_e, T_L	Electromagnetic and load torque
Ω	Rotor speed
ω_s, ω_r	Stator and rotor pulsation
θ_s, θ_r	Stator and rotor angular position
R_s	Stator resistance
R_r	Rotor resistance
L_s	Stator inductance
L_r	Rotor inductance
L_m	Mutual inductance
P	Number of pole pairs
J	Inertia
f	Friction factor

2. DFIM MODELING

2.1. Induction Machine Model

Assuming common simplifying assumptions, and applying Park transformation, the voltages equations of the induction machine expressed in the stator synchronous reference frame are given by [12]:

$$\begin{cases} V_{sd} = R_s I_{sd} + \frac{d\Phi_{sd}}{dt} - \omega_s \Phi_{sq} \\ V_{sq} = R_s I_{sq} + \frac{d\Phi_{sq}}{dt} + \omega_s \Phi_{sd} \\ V_{rd} = R_r I_{rd} + \frac{d\Phi_{rd}}{dt} - (\omega_s - \omega)\Phi_{rq} \\ V_{rq} = R_r I_{rq} + \frac{d\Phi_{rq}}{dt} + (\omega_s - \omega)\Phi_{rd} \end{cases} \quad (1)$$

The stator and rotor flux linkages may be written as:

$$\begin{cases} \Phi_{sd} = L_s I_{sd} + L_m I_{rd} \\ \Phi_{sq} = L_s I_{sq} + L_m I_{rq} \\ \Phi_{rd} = L_m I_{sd} + L_r I_{rd} \\ \Phi_{rq} = L_m I_{sq} + L_r I_{rq} \end{cases} \quad (2)$$

The mechanical equation

$$J \frac{d\Omega}{dt} = T_e - (f\Omega - T_L) \quad (3)$$

$$\omega = P\Omega \quad (4)$$

$$\frac{d\omega}{dt} = m_1 (I_{sq} I_{rd} - I_{sd} I_{rq}) - m_2 \omega - m_3 T_L \quad (5)$$

where: $m_1 = \frac{P^2 L_m}{J}$, $m_2 = \frac{f}{J}$, $m_3 = \frac{P}{J}$

The electromagnetic torque is given by:

$$T_e = P L_m (I_{sq} I_{rd} - I_{sd} I_{rq}) \quad (6)$$

The model of the DFIM in state space form with the six state variables: stator and rotor currents, speed and angular position, is given by [12].

$$\begin{bmatrix} I_{sd} \\ I_{sq} \\ I_{rd} \\ I_{rq} \\ \omega \\ \theta \end{bmatrix} = \begin{bmatrix} a_1 I_{sd} + (a\omega + \omega_s) I_{sq} + a_3 I_{rd} + a_5 \omega I_{rq} \\ -(a\omega + \omega_s) I_{sd} - a_1 I_{sq} - a_5 \omega I_{rd} + a_3 I_{rq} \\ a_4 I_{sd} - a_6 \omega I_{sq} - a_2 I_{rd} + (\omega_s - \omega/\sigma) I_{rq} \\ a_6 \omega I_{sd} + a_4 I_{sq} + \left(-\omega_s + \frac{\omega}{\sigma}\right) I_{rd} - a_2 I_{rq} \\ m_1 (I_{sq} I_{rd} - I_{sd} I_{rq}) - m_2 \omega \\ \omega \end{bmatrix} + \begin{bmatrix} b_1 & 0 & -b_3 & 0 & 0 \\ 0 & b_1 & 0 & -b_3 & 0 \\ -b_3 & 0 & b_2 & 0 & 0 \\ 0 & -b_3 & 0 & b_2 & 0 \\ 0 & 0 & 0 & 0 & 0 \\ 0 & 0 & 0 & 0 & -m_3 \end{bmatrix} \begin{bmatrix} V_{sd} \\ V_{sq} \\ V_{rd} \\ V_{rq} \\ \omega \\ \theta \end{bmatrix} \quad (7)$$

where : $\sigma = 1 - \frac{L_m^2}{L_s L_r}$, $a = \frac{1-\sigma}{\sigma}$, $a_1 = \frac{R_s}{\sigma L_s}$, $a_2 = \frac{R_r}{\sigma L_r}$, $a_3 = \frac{R_r L_m}{\sigma L_s L_r}$, $a_4 = \frac{R_s L_m}{\sigma L_s L_r}$, $a_5 = \frac{L_m}{\sigma L_s}$, $a_6 = \frac{L_m}{\sigma L_r}$, $b_1 = \frac{1}{\sigma L_s}$, $b_2 = \frac{1}{\sigma L_r}$, $b_3 = \frac{L_m}{\sigma L_s L_r}$

2.2. Matrix Converter Model

The matrix converter shown in Figure 2 is introduced for the first time by L. Gjugyi and B. Pelly [13]. This is a 3-phase/3-phase direct converter. The three phase input is directly connected to the phase output using nine bidirectional switches. This converter can produce a three-phase output voltage with variable amplitude and frequency (output voltage amplitude limited to 86% of the input [14]).

To control the matrix converter, we adopted the Scalar Alesina & Venturini technology. The principle of this technology is to synthesize the desired voltage three phase output from the input voltage for each switching period. In the same manner, the input currents are synthesized from the output currents. To establish the model of the matrix converter, we consider a balanced three phase input voltage V_i with the input pulsation ω_i and a balanced three phase output voltage V_o with the output pulsation ω_o as described respectively in (8) and (9).

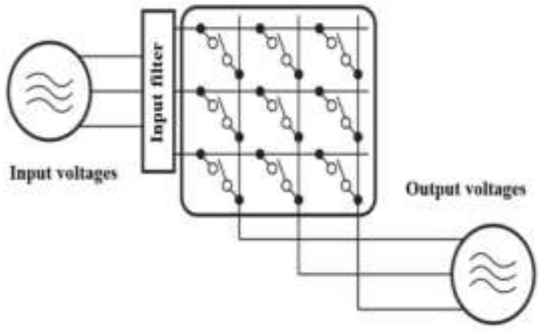

Figure 2. Matrix converter

$$V_i = \begin{bmatrix} V_{rn}(t) \\ V_{sn}(t) \\ V_{tn}(t) \end{bmatrix} = \begin{bmatrix} |V_i|\cos(\omega_i t) \\ |V_i|\cos(\omega_i t - \frac{2\pi}{3}) \\ |V_i|\cos(\omega_i t - \frac{4\pi}{3}) \end{bmatrix} \quad (8)$$

$$V_o = \begin{bmatrix} V_{un}(t) \\ V_{vn}(t) \\ V_{wn}(t) \end{bmatrix} = \begin{bmatrix} |V_o|\cos(\omega_o t + \theta_o) \\ |V_o|\cos(\omega_o t + \theta_o - \frac{2\pi}{3}) \\ |V_o|\cos(\omega_o t + \theta_o - \frac{4\pi}{3}) \end{bmatrix} \quad (9)$$

The input and output currents are given by:

$$I_i = \begin{bmatrix} I_r(t) \\ I_s(t) \\ I_n(t) \end{bmatrix} = \begin{bmatrix} |I_i|\cos(\omega_i t + \varphi_i) \\ |I_i|\cos(\omega_i t + \varphi_i - \frac{2\pi}{3}) \\ |I_i|\cos(\omega_i t + \varphi_i - \frac{4\pi}{3}) \end{bmatrix} \quad (10)$$

$$I_o = \begin{bmatrix} I_u(t) \\ I_v(t) \\ I_w(t) \end{bmatrix} = \begin{bmatrix} |I_o|\cos(\omega_o t + \varphi_o + \theta_o) \\ |I_o|\cos(\omega_o t + \varphi_o + \theta_o - \frac{2\pi}{3}) \\ |I_o|\cos(\omega_o t + \varphi_o + \theta_o - \frac{4\pi}{3}) \end{bmatrix} \quad (11)$$

The relationship between the output and the input voltages is defined by [15]:

$$V_o(t) = M(t) \cdot V_i(t) \quad (12)$$

Similarly, the relationship between the output and the input currents is defined as follows :

$$I_i(t) = [M(t)]^T I_o(t) \quad (13)$$

$M(t)$ is the conversion matrix which determines the state of the converter switches for each time period. It gives the nine duty cycles m_{jk} of the nine switches of the matrix converter.

3. DFIM CONTROL

3.1. Field Oriented Control

Vector control technique is used in the present study in order to ensure independent regulation of the speed and torque. Vector control, also called field-oriented control, stems from decoupled flux-current and torque-current control in AC drives. This in turns is similar to the principle of decoupled control of excitation and armature currents in DC machines [12].

In general, the FOC is used according to one of the following two ways. The one, known as indirect field oriented control (IFOC), proceeds by imposing a dynamic slip speed as derived from the equation of the rotor flux in order to ensure the orientation of the flux. The other way, known as direct field oriented control (DFOC), uses the measurement or estimation of the flux to get its magnitude and angle which is necessary for flux orientation. The indirect field oriented control is applied here for the control of the DFIM. In this case, the flux is not measured but defined by a preset value of its magnitude, and its angular position θ_s. This angle is obtained from the stator pulsation ω_s. The later is considered as the sum of the estimated rotor pulsation ω_r and the measured rotor speed ω (Figure 3). The stator flux orientation control used here consists in aligning the d-axis of the rotating reference frame to the stator flux space vector.

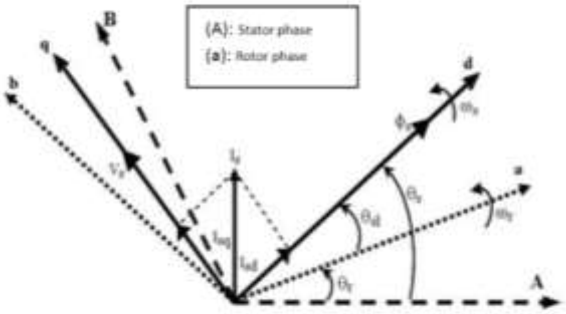

Figure 3. Orientation of the d- axis along the stator flux

By aligning the stator flux along the d- axis the components of the stator flux become:

$$\Phi_{sd} = \Phi_s \tag{14}$$

$$\Phi_{sq} = 0 \tag{15}$$

And by imposing a unity power factor at the stator, which leads to: $I_{sd} = 0$, the steady state equations governing the operation of the machine become as follows :

$$\begin{cases} V_{sd} = 0 \\ V_{sq} = R_s I_{sq} + \omega_s \Phi_{sd} \\ V_{rd} = R_r I_{rd} - (\omega_s - \omega_r)\Phi_{rq} \\ V_{rd} = R_r I_{rq} + (\omega_s - \omega_r)\Phi_{rd} \end{cases} \tag{16}$$

$$\begin{cases} \Phi_{sd} = L_m I_{rd} \\ \Phi_{sq} = 0 \\ \Phi_{rd} = L_r I_{rd} \\ \Phi_{rd} = -\frac{\sigma L_m}{1-\sigma} I_{sq} \end{cases} \tag{17}$$

The final expression of the electromagnetic torque is:

$$T_e = P L_m I_{sq} I_{rd} = P\,(\Phi_{sd} I_{sq}) \tag{18}$$

The compensation terms are applied according to the method introduced by D. Lecoq [16] which requires the use of four corrective currents. In order to get a good decoupling between d- and q- axis quantities, this method defines the new converted voltages as follows:

$$\begin{cases} V_{tsd} = V_{sd} - \frac{L_m}{L_r} V_{rd} \\ V_{trd} = V_{rd} - \frac{L_m}{L_s} V_{sd} \end{cases} \quad (19)$$

$$\begin{cases} V_{tsq} = V_{sq} - \frac{L_m}{L_r} V_{rq} \\ V_{trq} = V_{rq} - \frac{L_m}{L_s} V_{sq} \end{cases} \quad (20)$$

From (17) the q- and d-axis stator currents may be expressed as:

$$I_{sq} = -\frac{L_m}{L_s} I_{rq} \text{ and } I_{rd} = \frac{\Phi_{sd}}{L_m} \quad (21)$$

Also, from (19) and (20), it can be deduced :

$$\begin{cases} V_{tsd} = R_s I_{sd} + \sigma L_s \frac{dI_{sd}}{dt} - R_r \frac{L_m}{L_r} I_{rd} - \omega_s \Phi_{sq} + \frac{L_m}{L_r}(\omega_s - \omega)\Phi_{rq} \\ V_{tsq} = R_s I_{sq} + \sigma L_s \frac{dI_{sq}}{dt} - R_r \frac{L_m}{L_s} I_{rq} + \omega_s \Phi_{sd} - \frac{L_m}{L_r}(\omega_s - \omega)\Phi_{rd} \\ V_{trd} = R_r I_{rd} + \sigma L_r \frac{dI_{rd}}{dt} - R_s \frac{L_m}{L_s} I_{sd} - (\omega_s - \omega)\Phi_{rq} + \frac{L_m}{L_s}\omega_s \Phi_{sq} \\ V_{trq} = R_r I_{rq} + \sigma L_r \frac{dI_{rq}}{dt} - R_s \frac{L_m}{L_s} I_{sq} + (\omega_s - \omega)\Phi_{rd} - \frac{L_m}{L_s}\omega_s \Phi_{sd} \end{cases} \quad (22)$$

$$\begin{cases} V_{tsd} = V_{tsdc} + V_{tsdc1} = R_s I_{sd} + \sigma L_s \frac{dI_{sd}}{dt} + V_{tsdc1} \\ V_{tsq} = V_{tsqc} + V_{tsqc1} = R_s I_{sq} + \sigma L_s \frac{dI_{sq}}{dt} + V_{tsqc1} \\ V_{trd} = V_{trdc} + V_{trdc1} = R_r I_{rd} + \sigma L_r \frac{dI_{rd}}{dt} + V_{trdc1} \\ V_{trq} = V_{trqc} + V_{trqc1} = R_r I_{rq} + \sigma L_r \frac{dI_{rq}}{dt} + V_{trqc1} \end{cases} \quad (23)$$

where V_{tsdc1}, V_{tsqc1}, V_{trdc1} and V_{trqc1} denote the compensation terms. The diagram in Figure 4 shows the current controller and the voltage compensator which are cascaded in order to provide the reference voltage.

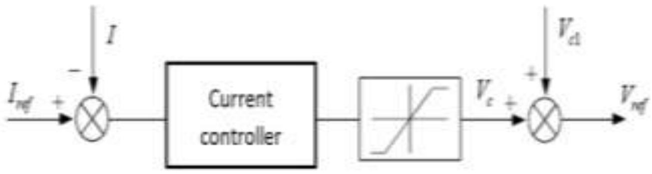

Figure 4. Current control diagram according to Lecocq method

The flux weakening is defined by the following expression:

$$\Phi_s = \begin{cases} \Phi_{sn} & \text{if } |\Omega| \le \Omega_N \\ \frac{\Omega_N}{|\Omega|}\Phi_{sn} & \text{if } |\Omega| > \Omega_N \end{cases} \quad (24)$$

3.2. The Adaptive Controller

In the present section the common PI controller and a fuzzy logic based PI controller are used and compared. The latter, which results from the combination of a PI controller and the fuzzy logic technique, named here adaptive controller (Adaptive PI), takes advantages of the fuzzy logic technique to provide an automatic tuning of the PI controller.

Due to their simplicity and low cost PI controllers are widely used in industrial applications. However, these simple analog controllers are linear and cannot control systems with varying parameters. Fuzzy logic (FLC) based controllers have non-linear structure with good performance and higher robustness in the control of non linear and varying parameters systems. In contrast, they have the drawback that they require a lot of information to account for the non-linearity when parameters change. Furthermore, if the number of FLC entries increase the size of the rules base increases [17].

The adaptive PI technique uses fuzzy logic to adjust the parameters of the PI controller (kp, ki) when the parameters of the controlled system change. This makes it adaptable for controlling nonlinear systems. The block diagram of this technique is illustrated in Figure 5.

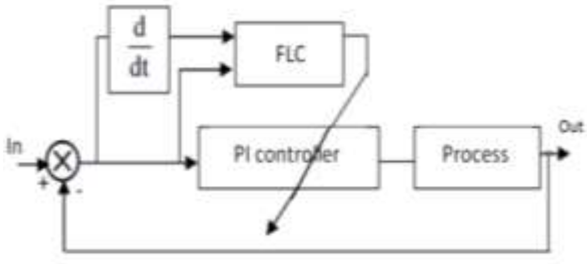

Figure 5. Principle of PI parameters tuning using fuzzy logic

The parameters of the PI controller are taken normalized in the range [0, 1], by using the following linear transformations [17]:

$$K_p' = (K_p - K_{pmin})/(K_{pmax} - K_{pmin}) \quad (25)$$

$$K_i' = (K_i - K_{imin})/(K_{imax} - K_{imin}) \quad (26)$$

Fuzzy logic controller inputs are: the error e and the error derivative de, the outputs are the normalized value of the proportional action K_p' and the normalized value of the integral action K_i'. The fuzzy sets of input variables are defined as follows: NB: Negative Big, NM: Negative Average, NS: Negative Small, Z: Zero, PS: Positive Small, PM: Positive Average and PB: Positive Big. The fuzzy sets of output variables are defined as follows: B: Big and S: Small. The membership functions for the inputs; e and de are defined in the range [-1, 1] (Figure 6) and the membership functions for the outputs are defined in the interval [0,1] (Figure 7).

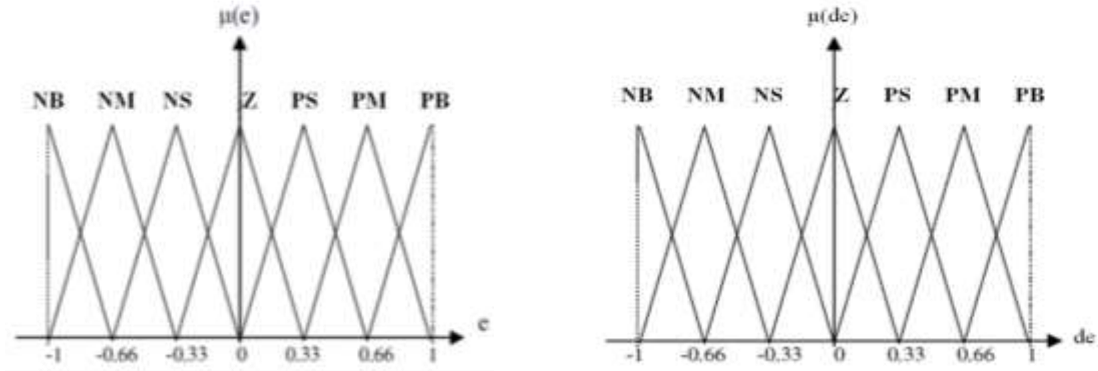

(a) (b)

Figure 6. Membership functions: (a) for e, (b) for de

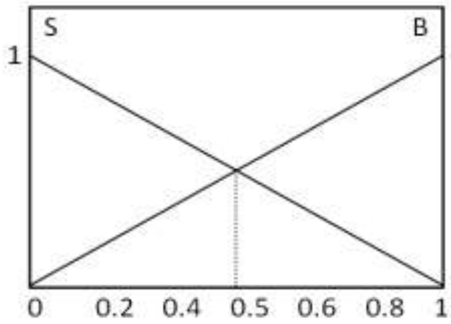

Figure 7. Membership function for K_i' and K_p'

The rules bases to calculate the parameters K_p' and K_i' are shown in Tables 1 and Table 2.

Table 1. Rule base for the output K_p'

e \ de	NB	NM	NS	Z	PS	PM	PB
NB	B	B	B	B	B	B	B
NM	S	B	B	B	B	B	B
NS	S	S	B	B	B	S	S
Z	S	S	S	B	S	S	S
PS	S	S	B	B	B	S	S
PM	S	B	B	B	B	B	S
PB	B	B	B	B	B	B	S

Table 2. Rule base for the output K_i'

e \ de	NB	NM	NS	Z	PS	PM	PB
NB	B	B	B	B	B	B	B
NM	B	B	S	S	S	B	B
NS	B	B	B	S	B	B	B
Z	B	B	B	S	B	B	B
PS	B	B	B	S	B	B	B
PM	B	B	S	S	S	B	B
PB	B	B	B	B	B	B	B

Once the values of K_p' and K_i' are obtained, the new parameters of the PI controller (K_p and K_i) are calculated by:

$$K_p = (K_{pmax} - K_{pmin})/K_p' - K_{pmin} \tag{27}$$

$$K_i = (K_{imax} - K_{imin})/K_i' - K_{imin} \tag{28}$$

4. SIMULATION RESULTS AND DISCUSSIONS

The used wound rotor induction machine has the following specifications.

Table 3. Specifications of the induction machine

Parameters	Values	
Nominal power	1.5	KW
Nominal speed	1450	tr/min
Number of pole pairs	2	-
Inertia	0.01	kgm²
Friction factor	0.0027	N.m.s
Nominal stator voltage	220	V
Nominal rotor voltage	130	V
Nominal stator current	4.3	A
Nominal rotor current	4.5	A
Nominal stator frequency	50	Hz
Nominal rotor frequency	50	Hz
Stator resistance	1.75	Ω
Rotor resistance	1.68	Ω
Stator inductance	295	mH
Rotor inductance	104	mH
Mutual inductance	165	mH

4.1. Speed Control

The simulations were performed under Matlab / Simulink environment. The simulation results presented and discussed below are obtained from tests applied to the DFIM powered by two matrix converters under IFOC. The DFIM is operated in motor mode.

The cycle of operation considered here is as follows:

a. A no-load starting of the machine is made with speed set point of 100 rd/s,
b. External disturbance is introduced by applying the rated load of 9 Nm, at t = 1s,
c. The load is removed at t = 1.75s,
d. The direction of rotation is reversed at t = 2.5s,
e. Changeover to a low speed (2.5% of nominal speed) at t = 3.25s,
f. The nominal load is applied at t = 4s.

According to the results obtained in Figure 8, we see that the DFIM speed follows well the reference speed all through the operating cycle; at startup, during the application and removal of the load, but also in the case of speed reversal. It can also be noticed that the effect of inertia (speed overshoot) is much less in the case of adaptive PI compared to classic PI controller. Also, at very low speed, the DFIM was able to overcome the nominal torque while following a reference of 2.5% the nominal speed. Moreover, it should also be noted that this high dynamic performance is made possible also thanks to the used FOC technique which ensures a dynamic torque response and a good decoupling between flux and torque. As can be seen on Figure 8d, the flux is maintained at its desired value through all the different phases of the operating cycle.

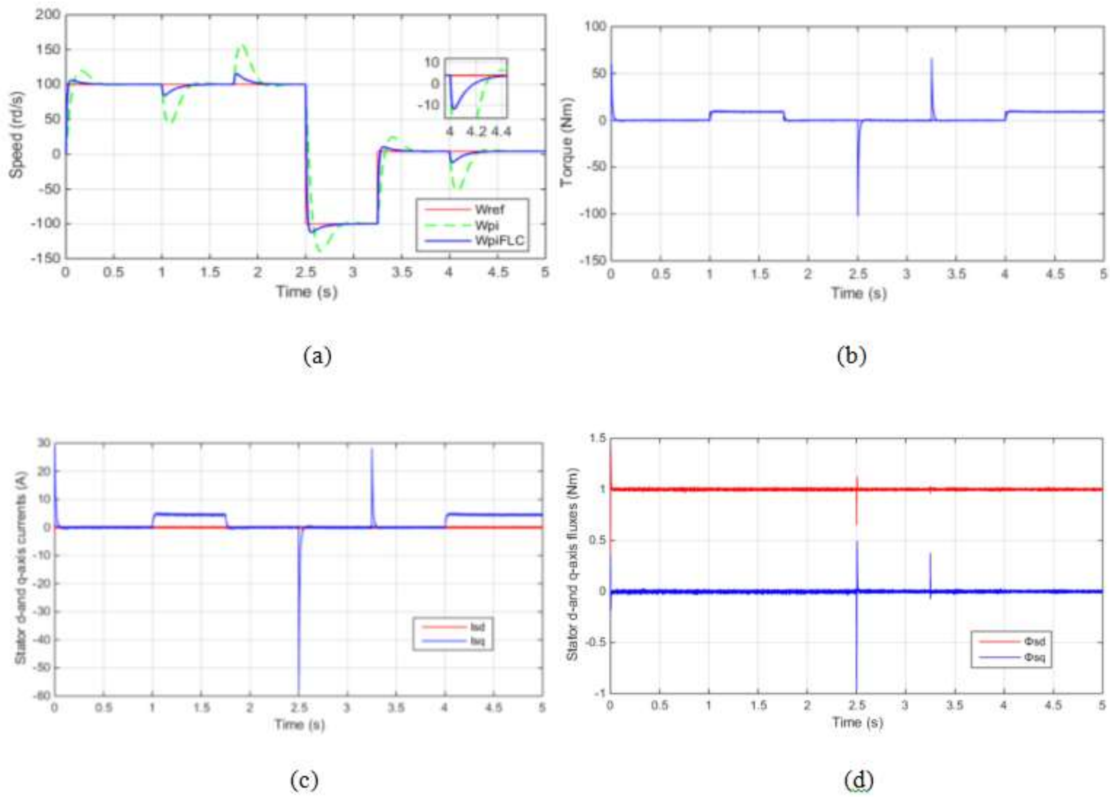

Figure 8. Simulation results of DFIM controlled by adaptive PI-FLC controller. (a) Speed, (b) Torque, (c) Stator currents, (d) Stator flux

4.2. Operation beyond the Nominal Power

In order to point out a very interesting and useful capability of the DFIM, another cycle of operation is considered as follows:

a. A no-load starting of the machine is performed with speed set point of 157 rd/s (nominal speed),
b. At time t=1s a load equal to twice the nominal load is applied
c. From time t=2s to t=3s the machine is running at no-load
d. At t=3s the speed is increased to twice the rated speed

e. The nominal load is applied at t=4s.
f. The load is removed at t=5s.

Figure 9 shows two types of overload operation of the DFIM. For instance, from time t=4s to t=5s the machine is driven at twice its rated speed while keeping the load torque at nominal value. Hence, in such situation, the DFIM is developing the double of its nominal power. This ability of the DFIM to overcome significant transient overloads is very useful in several industrial applications such as in mining and electric vehicle industries.

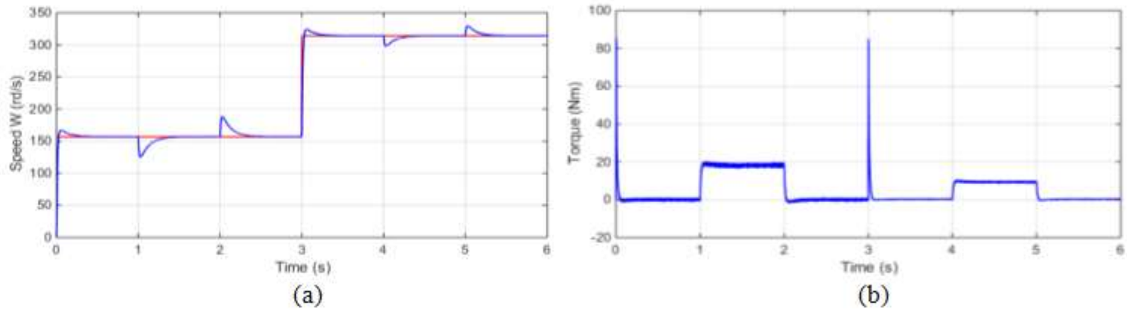

Figure 9. Simulation results of DFIM operation at twice rated power. (a) Speed, (b) Torque

4.3. Robustness Test

The main objective of these tests is to verify the performance of the DFIM control with respect to variations of its parameters. Various tests were carried out by performing machine parametric variations and this up to 50% for stator and rotor resistors, and also up to 50% for the inertia. The tests were performed according to the following operating cycle: Starting at no load with a speed set point of 100rd/s at time t=0, then, variations in machine parameters are applied at time t=0.5s, and finally the speed is reversed and set to-100rd/s at t=3s. The load torque is applied t=1s and then removed at t=2s. Observing the results shown in Figure 10, it is obvious that changes in machine parameters did not influence the proper functioning of the DFIM, which confirms the robustness of the control technique.

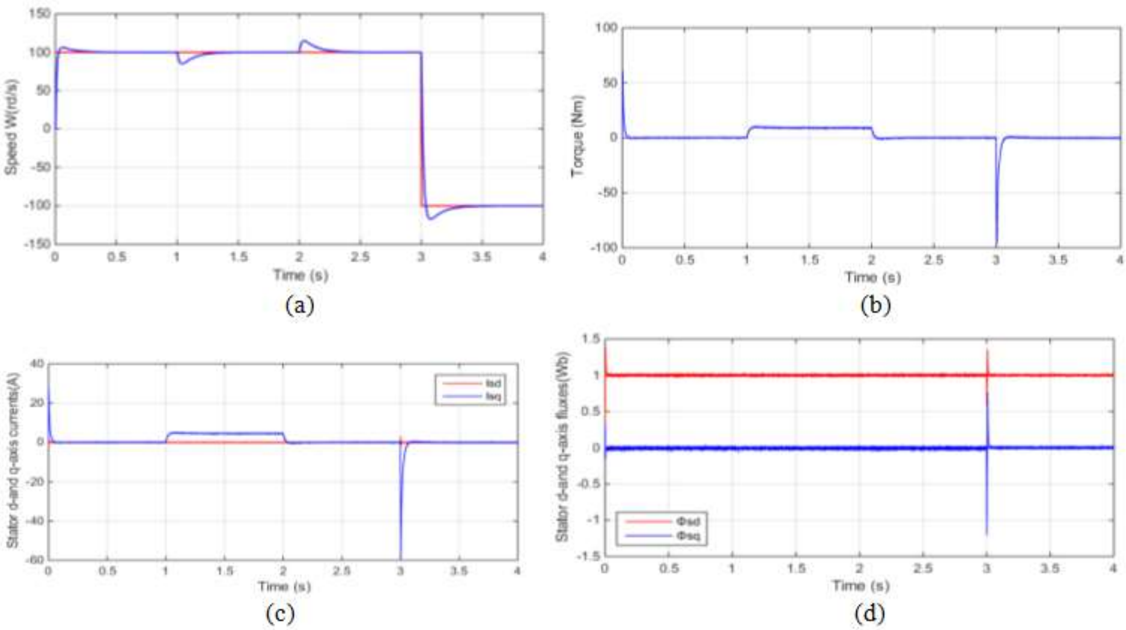

Figure 10. Robustness test of the adaptive PI-FLC controller with respect to stator and rotor resistances and the inertia of the DFIM. (a) Speed, (b) Torque, (c) Stator currents, (d) Stator flux

5. CONCLUSION

In this article we studied the DFIM associated with two matrix converters respectively connected to the stator and rotor windings. The obtained results show that the DFIM responds favorably to speed and torque demand. Due to the good decoupling provided by vector control technique, the flux and speed follow accurately their references. The simulation results show a remarkable behavior of the adaptive PI controller when compared to that of conventional PI. Also, it should be noted the high performance offered by the adaptive PI controller regarding the robustness. Finally, we simulated a very severe operation which consists to operate the DFIM beyond its rated power. In fact, the speed was doubled while keeping the torque at its nominal value. The DFIM has responded favorably to this request, and consequently was able to provide a power equal to twice its rated power. This can be very useful to overcome a significant transient overload. However, we must consider the overheating generated during this operation.

REFERENCES

[1] A.B. Asuhaini, B.M. Zin, M.H.A. Pesaran, A.B. Khairuddin, "An overview on doubly fed induction generators control and contributions to wind based electricity generation", *Renewable and Sustainable Energy Reviews*, vol. 27, pp. 692–708, November 2013.

[2] Md Maruf Hossain, Mohd. Hasan Ali, "Future research directions for the wind turbine generator system”, *Renewable and Sustainable Energy Reviews*, vol. 49, pp. 481–489, September 2015.

[3] M. Liserre, R. Cardenas, M. Molinas, J. Rodriguez, "Overview of multi-MW wind turbines and wind parks”, *IEEE Trans. Ind Electron*, vol. 58, pp. 1081-1095, April 2011.

[4] Ming Cheng, Ying Zhu, "The state of the art of wind energy conversion systems and technologies: a review", *Energy Conversion and Management*, vol. 88, pp. 332–347, December, 2014.

[5] Hüseyin Altun, Sedat Sünter, "Modeling, simulation and control of wind turbine driven doubly-fed induction generator with matrix converter on the rotor side", *Electrical Engineering*, Springer, vol. 95, pp.157-170, June 2013.

[6] F. Bonnet, M. Pietrzak-David, “Control optimization of a Doubly Fed Induction Machine”, *IEEE Power Electronics Specialists Conference*, Rhodes, 15-19 June 2008, pp. 2579 – 2585.

[7] R.Babouri, D.Aouzellag, K.Ghedamsi, "Introduction of Doubly Fed Induction Machine in an Electric Vehicle", *Energy Procedia*, vol. 36, pp.1076 – 1084, 2013.

[8] Paweł Szcześniak, Jacek Kaniewski, "Power electronics converters without DC energy storage in the future electrical power network”, *Electric Power Systems Research*, vol. 129, pp. 194–207, December 2015.

[9] J. Karpagam, A. Nirmal Kumar, V. Kumar Chinnaiyan, M. Surya, Implementation of Direct Torque Control for Matrix Converter Fed Induction Motor Drive Using Fuzzy Logic Controller, *Power Electronics and Renewable Energy Systems*, Springer, pp. 383-393, 2014.

[10] Youcef Soufi, Tahar Bahi, Salima Lekhchine, Djalel Dib, Performance analysis of DFIM fed by matrix converter and multi level inverter, *Energy Conversion and Management*, vol. 72, pp. 187–193, August 2013.

[11] Alireza Jahangiri, Ahmad Radan, "Indirect matrix converter with unity voltage transfer ratio for AC to AC power conversion”, *Electric Power Systems Research*, vol. 96, pp. 157–169, March 2013.

[12] B. K. Bose, Modern power electronics and AC drives, Prentice-Hall, 2002.

[13] L. Gjugyi, B. Pelly, Static Power Frequency Changers, New York: Wiley, 1976.

[14] A. Alesina, M. Venturini : "Analysis and Design of Optimum-Amplitude Nine Switch Direct AC-AC Converters", *IEEE Transactions Power Electron*., vol.4, no.1, pp. 101-112, January 1989.

[15] A. Alesina, M. Venturini, "Solid-State Power Conversion: A Fourier Analysis Approach to Generalized Transformer Synthesis", *IEEE Transactions on circuits and systems*, vol. 28, issue 4, pp. 319-330, April 1981.

[16] Georges Salloum, “Contribution à la Commande Robuste de la Machine Asynchrone à Double Alimentation”, Ph.D. dissertation, Toulouse Univ., Toulouse, France, 2007.

[17] B. Hamane, M.L. Doumbia, M. Bouhamida, M. Benghanem , “Control of wind turbine based on DFIG using Fuzzy-PI and Sliding Mode controllers”, *Proc. of Ninth International Conference on Ecological Vehicles and Renewable Energies (EVER)*, Monte-Carlo, 25-27 March 2014, pp.1-8.

[18] G. Venu Madhav, Y.P. Obulesu ‘A Fuzzy Logic Control Strategy for Doubly Fed Induction Generator for Improved Performance under Faulty Operating Conditions’, *International Journal of Power Electronics and Drive System (IJPEDS)*, Vol. 4, No. 4, December 2014, pp. 419-429.

[19] Pritha Agrawal, Satya Prakash Dubey, Satyadharma Bharti ‘Comparative Study of Fuzzy Logic Based Speed Control of Multilevel Inverter fed Brushless DC Motor Drive’, *International Journal of Power Electronics and Drive System (IJPEDS)*, Vol. 4, No. 1, March 2014 pp. 70-80.

BIOGRAPHIES OF AUTHORS

Abdelhakim Alalei received his M.Sc. degree in electrical engineering from the Electrical Engineering Institute of the University of Bechar, Algeria in 2013. He is currently working towards his Ph.D at Bechar University with research interests relating to power electronics, electric machines and modern controllers. Alalei's research focuses on the control of DFIM powered by matrix converters.

Hazzab Abdeldjebar received his State Engineer, M.S., and Ph.D degrees in Electrical Engineering from the Electrical Engineering Institute of The University of Sciences and Technology of Oran (USTO), Algeria in 1995, 1999, and 2006, respectively. He is currently a Professor of Electrical Engineering at the University of Bechar (Algeria), where he has been the Director of the Research Laboratory of Command, Analyses, and Optimization of Electro-Energetic Systems since 2009. His research interests include power quality, modeling, modern controller and observer design for nonlinear systems, control of power electronics, multidrive systems and electrical vehicle, and adaptive control and nonlinear systems diagnostic.

Ali Nesba received the BSc, MSc and PhD degrees in electrical engineering from the National Polytechnic School of Algiers, Algeria. Since 2002, he joined the department of computer science of the "Ecole Normale Supérieure de Kouba," Algiers, Algeria, where he is a professor of electrical engineering and director of the LSIC research Lab. His research interests include electric machines, power electronics and renewable energy systems.